Available online at http://www.ssstj.sci.ssru.ac.th

Suan Sunandha Science and Technology Journal

Synthesis of Copper Nanoparticles-polyvinylpyrrolidone Composite Materials Using Simultaneous Irradiation Process

Thanawat Kasemsankidakarn[1,2], Parichart Kongkaoroptham[2], Thananchai Piroonpan[2], Wanvimol Pasanphan[1,2*]

[1]Department of Materials Science, Faculty of Science, Kasetsart University, 50 Ngam Wong Wan Rd., Ladyao, Chatuchak, Bangkok 10900, Thailand

[2]Center of Radiation Processing for Polymer Modification and Nanotechnology (CRPN), Faculty of Science, Kasetsart University, 50 Ngam Wong Wan Rd., Ladyao, Chatuchak, Bangkok 10900, Thailand

*Corresponding author e-mail: wanvimol.p@ku.ac.th

Received: *28 February 2022* / **Revised**: *16 March 2022* / **Accepted**: *14 June 2022*

Abstract

An approach for the synthesis of copper nanoparticles (CuNPs) embedded in poly (vinylpyrrolidone) (PVP) composite materials is proposed using a simultaneous irradiation process. The parameters, i.e., copper sulfate (CuSO4) precursor, VP and PVP concentrations were optimized for synthesis of CuNPs under irradiation. Crosslinking of PVP system was analyzed by gel fraction and swelling degree using gravimetric measurement. Functionality, chemical composition and crystallinity of the CuNPs-PVP composite materials were characterized by FT-IR, SEM-EDS, XRD. Morphology of the CuNPs-PVP composite materials was observed using SEM. Light blue color of Cu^{2+} precursor in liquid polymer/monomer system changed to dark brown color of Cu in solid form. Stable CuNPs with the particle diameters ranging from ca.100 to 500 nm was successfully synthesized in the PVP solid materials. A simple and effective process for the preparation of the CuNPs-PVP composite materials serves as a new generation of process and functional nanomaterials for industrial applications.

Keywords: Copper nanoparticles, Poly (vinylpyrrolidone), Nanocomposite, Irradiation

1. Introduction

Copper nanoparticles (CuNPs) are metal materials in a nano-sized scale (<100 nm) having high surface area to volume ratio resulting in strong electrical conductivity (Athanassiou, Grass, & Stark, 2006) catalytic property and antibacterial activity (Wahyudi, Soepriyanto, Mubarok, & Sutarno, 2018). CuNPs are considered as one of the alternative materials for replacing other bulk metallic materials because it has lower price than gold and silver, etc., (Cheng et al., 2017; Tomotoshi & Kawasaki, 2020). For example, it has been used as conductive fabrics (Moazzenchi & Montazer, 2020), catalysts, antibacterial agents and pigments (Athanassiou et al., 2006) in various applications. In case of soldering connections, conductive paste has valuable applications in the electronic industry, such as printed circuits and circuit repair (Zinn et al., 2012). However, CuNPs have high oxygen sensitivity which will then aggregate and be readily oxidized by oxygen in an aqueous environment, high humidity and air environment (Wahyudi et al., 2018). Therefore, several strategies for the synthesis of CuNPs by reducing oxidation in order to develop stable CuNPs for desirable applications is still in the line of scientific and technological development.

Many approaches for synthesizing CuNPs are based on the reduction process of Cu(II) ions as a precursor to CuNPs. Up to present, the process for the synthesis of CuNPs includes chemical reduction using various chemical reducing agents (Chandra, Kumar, & Tomar, 2014), photo-induced reduction (Giuffrida, Costanzo, Ventimiglia, & Bongiorno, 2008), sonochemical (Wongpisutpaisan, Charoonsuk, Vittayakorn, & Pecharapa, 2011) and

Suan Sunandha Science and Technology Journal

radiolytic methods (Zhou et al., 2008). The benefits of radiolytic synthesis of metal NPs are chemical reducing agent free, size controllable, simultaneous reaction and fabrication, practical, and easiness (Flores-Rojas, López-Saucedo, & Bucio, 2020). Ionizing radiations generate the reactive species (e.g., solvated electrons, ions and free radicals) in a controlled synthetic system. The solvated electrons have an incredibly negative redox potential and they play an important role as a source of reducing agent to promote reduction reaction (Joshi, Patil, Iyer, & Mahumuni, 1998). This brings about the phenomena causing reduction of metal ions to their zero valent state. Metal cluster properties are often affected by the interaction between the metal and the surrounding molecules (e.g., solvent, ligand, stabilizer). In contrast to chemical reduction of metal ions, the radiation chemical process for colloid preparation has significant benefits in that there are no irritating impurities such as chemical reducing agents. Radiolysis process produces pure and enables the creation of stable nanoparticles by controlling the stabilizer and irradiation synthesis system (Flores-Rojas et al., 2020). Radiolysis process have been proposed for the synthesis of silver nanoparticles (Jannoo, Teerapatsakul, Punyanut, & Pasanphan, 2015; Ramnani, Biswal, & Sabharwal, 2007), gold nanoparticles (Bondaz et al., 2020; Meyre, Tréguer-Delapierre, & Faure, 2008) and copper nanoparticles (Ahmad, Ahmad, & Radiman, 2009; Alyan, Abdel-Samad, Massoud, & Waly, 2019).

It is known that polymer stabilizer is an important component for stabilizing metallic nanoparticles not only during the synthesis process but also prolonging the post-synthesized product. Polymers containing reactive functions for providing strong complexation or coordination and electrostatic interaction with the metallic ions precursor and their nanoparticles have been considered as stabilizers for metallic nanoparticle synthesis. Chitosan and its derivatives (Tangthong et al., 2021a, 2021b), silk fibroin peptide (Wongkrongsak, Tangthong, & Pasanphan, 2016), ascorbic acid (Ismail et al., 2019), polyvinyl alcohol (PVA) (Zhou et al., 2008) and polyvinyl pyrrolidone (PVP) (Misra, Biswal, Gupta, Sainis, & Sabharwal, 2012) have been used as polymer stabilizer for metallic NPs synthesis. PVP is an amorphous, hygroscopic synthetic polymer composed of linear 1-vinyl-2-pyrrolidinone function (Hiremath, Nuguru, & Agrahari, 2019). During the nanoparticle synthesis, PVP could form a protective layer on the surface of various nanoparticles (Hsu & Wu, 2007). N-vinylpyrrolidone (VP) is a hydrophilic monomer of PVP that is commonly used as a stabilizer for polymer-based nanoparticles (Pornpitchanarong, Rojanarata, Opanasopit, Ngawhirunpat, & Patrojanasophon, 2020). PVP helps to resist aggregation by possessing a steric hindrance structure and acting as NPs dispersant when formulated into a polymer matrix. This leads to the ability to formulate metallic NPs with remarkably stable and inert properties (Koczkur, Mourdikoudis, Polavarapu, & Skrabalak, 2015). To the best of our knowledge, a simultaneous synthesis of CuNPs in solid PVP polymer using radiolysis method has not yet been reported.

In this work, we are, therefore, focusing on the synthesis and fabrication of CuNPs in PVP solid matrix using simultaneous gamma-ray irradiation process. The effects of PVP, VP, and Cu precursor concentrations on radiolytic synthesis of CuNPs in PVP composite were studied. Chemical structures were characterized by Fourier Transform Infrared Spectroscopy (FT-IR). CuNPs formation was confirmed by X-rays Diffraction (XRD). The elemental composition of CuNPs in PVP composite materials were observed by Energy Dispersive X-rays Spectrometer (SEM/EDS). Stability of CuNPs-PVP composite materials was investigated within a time interval.

2. Materials and Methods

2.1 Materials

Copper (II) sulfate ($CuSO_4$, MW = 159.6 Da) was purchased from Ajax Finechem Pty Ltd. (Australia). Poly (vinyl pyrrolidone) (PVP) K-30 (MW = 40,000 g/mol) and vinyl pyrrolidone (VP, MW = 111.14 g/mol) were bought from Guangdong Yumay Chemical Co., Ltd. (China).

Suan Sunandha Science and Technology Journal

2.2 Instrument and characterizations

Gamma-rays irradiation process was carried out in a ^{60}Co Gammacell 220 irradiator with a dose rate of 1.6 kGy/h. A Red-dyed PMMA dosimeter type Red 4304 was supplied from Harwell Dosimeter Ltd. The samples were irradiated in air under room temperature and pressure. FTIR analyses were carried out by Fourier Transform Infrared Spectroscopy (FT-IR) in Bruker Tensor 27 (USA) with Attenuated Total Reflectance Mode (ATR mode). The FTIR spectra detected 32 scans at a resolution of 2 cm^{-1} in a frequency range of 4000-400 cm^{-1}. The X-ray diffraction (XRD) patterns were taken on a Bruker AXS (Germany) with CuK_{α} radiation as an X-ray source operating at 50 kV and 100 mA. The diffraction data were collected over the angular 2θ range of 10-80° at a scan rate of 5°/min. A standard powder diffraction card of JCPDS, copper file (No. 01-1241 & 03-1005) (Ramesh, Vetrivel, Suresh, & Kaviarasan, 2020) was used for identifying the characteristic diffraction. Morphology and elemental composition of the composite were assessed using scanning electron microscope with Scanning Electron Microscope - Energy Dispersive X-rays Spectrometer (SEM/EDS) in Quanta 450, FEI (Netherlands). The samples were cut into rectangular shape and then placed onto carbon tape on an aluminum holder. Physical appearance and stability were carried out under room temperature by CanoScan LiDE 300 scanner. The recorded data were observed for 0, 7 and 180 days.

2.3 Synthesis of CuNPs in PVP-VP composite materials by gamma-rays irradiation process

$CuSO_4$ solution (6.384 g, 400 mM) was prepared by dissolving in distilled water (100 mL). The $CuSO_4$ solution (400 mM, 0, 250, 500, 750, 1000 µL) were mixed with PVP powder (0, 2, 4, 6, 8 g). VP solution was then added to adjust final concentration $CuSO_4$/PVP/VP mixture for 10 mL to obtain the mixtures with $CuSO_4$ (0, 10, 20, 30 and 40 mM) and PVP (0, 10, 20, 30 and 40% w/w) in VP (50-100% w/w). The mixtures were irradiated by gamma-rays irradiation with an absorbed dose of 25 kGy in air under room temperature to obtain CuNPs in polymerized VP in PVP (CuNPs/PVP-VP_n). Similarly, PVP matrix without $CuSO_4$ was also prepared. PVP powder (1, 2, 3, 4, 5 and 6 g) were mixed with VP solution (9, 8, 7, 6, 5 and 4 g) to obtain the total volume of 10 g of PVP-VP solution with various concentrations of PVP 10, 20, 30, 40, 50 and 60% w/v, respectively. The solution was vigorously stirred for 4 h and then irradiated by gamma-rays at 25 kGy in air under room temperature to obtain polymerized VP in PVP (PVP-VP_n) matrix.

FTIR (ATR, cm^{-1}) for PVP (Fig. 3(a)): 3450 (O-H stretching), 2941 (C-H stretching), 1648 (C=O stretching), 1420, (C-N stretching) 1285 (C-N bending), 840 (pyrrolidone ring), 646, 567 (N-C=O bending). For VP (Fig. 3(b)): 2941 (C-H stretching), 1693 (C=O stretching), 1625 (C=C stretching), 1420, (C-N stretching), 1285 (C-N bending), 840 (pyrrolidone ring), 646, 567 (N-C=O bending). For PVP/VP mixture (Fig. 3(c)): 2941 (C-H stretching), 1693 (C=O stretching), 1625 (C=C stretching), 1423 (C-N stretching), 1285 (C-N bending), 840 (pyrrolidone ring), 646, 567 (N-C=O bending). For irradiated PVP-VP (25 kGy) (Fig. 3(d)): 3450 (O-H stretching), 2941 (C-H stretching), 1648 (C=O stretching), 1423 (C-N stretcing), 1285 (C-N bending), 840 (pyrrolidone ring), 646, 567 (N-C=O bending).

2.4 Gel fraction analysis of PVP-VP_n

The irradiated samples were dried at 60ºC in an air-oven for 48 h and cut into the dimension of 1 × 1 cm^2. Piece of sample was immersed in distilled water (50 mL) at room temperature within a time interval of 0-168 h. The sample was taken out from the solution and then dried at 60ºC in air oven for 48 h. Gel fraction were determined from (W_d/ W_i) × 100, where W_i is an initial weight of dried sample before immersing in water and W_d is a weight of dried water-insoluble gel.

Suan Sunandha Science and Technology Journal

2.5 Swelling behavior of PVP-VP_n

The insoluble gel samples were dried at 60ºC in an air-oven for 48 h and cut into the dimension of 1×1 cm^2 and immersed in distilled water (50 mL) at room temperature. The swollen samples were taken out from solution and weight within time interval of 0-168 h. The swollen samples were dried at 60ºC in air oven for 48 h and then weight to obtain a weight of dried water-insoluble gel (W_d). The swelling degree was calculated from $((W_s - W_d)/W_d) \times 100$, where W_d is a weight of dried insoluble gel and W_s is a weight of swollen gel.

3. Results and Discussion

Formation of CuNPs in PVP-VP_n was simultaneously synthesized and fabricated using radiolysis-based mechanism via radiation-induced reduction and radiation-induced polymerization/crosslinking. Under irradiation, the primary reactive species, i.e., electron from ionization (e^-), excited molecule (R^*) and ions ($R^{\bullet+}$) were generated. Dissociation of excited molecules then brought about free radical production, such as macro radical ($R^\bullet$) of polymer and hydroxyl radical ($H^\bullet$). The $H^\bullet$ and $R^\bullet$ undergo initiation, polymerization and crosslinking of VP and PVP system to create PVP-VP_n solid matrix. Meanwhile, the solvate electron play an important role in the reduction of copper ions (Cu^{2+}) to copper atom (Cu^0) for the production of CuNPs. Radiation-induced reaction of Cu^{2+} for CuNPs synthesis are similar to that of AuNPs and AgNPs as in the previous reports (Jannoo et al., 2015; Piroonpan, Katemake, & Pasanphan, 2020).

3.1 Gel formation of PVP-VP_n matrix

The effect of PVP-VP_n concentration on gel fraction is shown in Figure 1. The PVP-VP_n solid matrix was prepared by gamma-rays irradiation with a dose of 25 kGy. With increasing PVP concentration in the VP liquid monomer, it was found that the gel fraction gradually reduced. The gel fraction was reduced from 59.62% to 32.46% and 20% wt%, when the concentration of PVP increased from 0 to 10 and 20 %wt. The gel fraction decreased down to zero when the PVP concentration was higher than 30 %wt. The results indicated that PVP influenced gel formation in the PVP/VP system. Increasing PVP in VP obstructs the polymerization of VP to VP_n and VP_n might be grafted or crosslinked on the PVP polymer chain. By increasing PVP, in other word reducing VP, the amount of reactive vinyl function of VP also reduced and gel fraction tended to decline. Although the PVP-VP_n became solid form, part of the obtained PVP-VP_n matrix was in a water-soluble form.

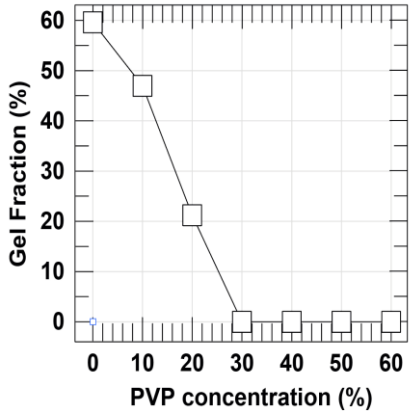

Figure 1. Gel fraction of PVP-VP_n material prepared using different PVP concentrations and irradiated at an absorbed dose of 25 kGy.

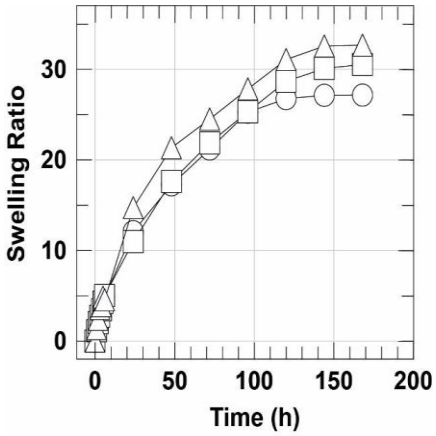

Figure 2. Swelling ratio of PVP-VP_n material prepared using differnt PVP concentration or with PVP: VP ratio of 0:100 (○), 10:90 (□), and 20:80 (△) and irradiated at 25 kGy.

Suan Sunandha Science and Technology Journal

3.2 Kinetics swelling of PVP-VP_n matrix

Kinetic swelling of PVP-VP_n was analyzed as shown in Figure 2. Swelling behavior of PVP-VP_n having gel formation was used for observing the swelling ratio. According to the gel fraction result, the PVP-VP_n with the PVP: VP ratio of 0: 100, 10: 90 and 20: 80 were selected. The swelling ratio of all PVP-VP_n samples increased within the time interval of 0-168 h. By prolonging the immersion time, the swelling ratio increased from 0 to around 30%. The swelling ratio of all samples reached a steady state at 168 h (7 days). The greater the gel fraction, the lower swelling ratio was observed because network formation in the PVP-VP_n structure obstructed the expansion of PVP-VP_n chains.

3.3 Functional groups characterization

The functional groups of PVP-VP_n were characterized by FTIR as shown in Figure 3. FIIR spectrum of PVP shows peak at 1648 cm^{-1} assigned to carbonyl group (C=O) on the PVP ring, 3450 and 2941 cm^{-1} assigned to O–H and C–H stretching. Other significant bands of PVP include those caused by pyrrolidone ring at 840 cm^{-1} and N-C=O bending at 567 cm^{-1}. In the case of VP (Figure 3(b)), the peak at 1625 cm^{-1} interpreted as C=C stretching was significantly observed. When PVP was mixed with VP (Figure 3(c)), the C=C stretching peak of VP was additionally found when compared with PVP (Figure 3(a)). After irradiation with the dose of 25 kGy, the characteristic vinyl peak at 1625 cm^{-1} disappeared from the FTIR spectrum of the irradiated PVP-VP_n spectrum (Figure 3(d)). An absence of the C=C absorption band in the irradiated PVP-VP sample suggests that the VP monomer was converted to C-C bond owing to polymerization process upon irradiation.

3.4 Morphology and element analysis

Physical appearance, morphologies and elemental mapping profile of the representative PVP-VP_n and CuNPs-PVP-VP_n composite presented in Figure 4. PVP-VP_n matrix exhibited transparent and light-yellow color in a solid form (Figure 4A(a)). With the CuNPs constructed in the PVP-VP_n matrix, color was changed to be dark brown or copper-like color (Figure 4A(b)). Generally, the color of Cu^{2+} before irradiation was blue due to the characteristic color of $CuSO_4$ (data not shown). Therefore, change of color from blue to copper-like implies the formation of CuNPs due to transformation of Cu^{2+} to Cu^0 atoms upon radiation-induced reduction mechanisms. Figure 4B shows their corresponding SEM images of PVP-VP_n and CuNPs-PVP-VP_n composite samples. The surface morphology of PVP-VP_n was smooth and clear without any particular composite in the matrix. On the other hand, CuNPs-PVP-VP_n samples evidently displayed embedded CuNPs in the PVP-VP_n matrix. The particle size of CuNPs was mostly observed to be ca.100 nm and somewhat agglomerated particles with the size ca. 500 nm was also found in the PVP-VP_n matrix. The morphological information from SEM images implied that CuNPs was successfully synthesized in the PVP-VP_n matrix.

To observe the presence of the Cu element in the PVP-VPn matrix, SEM-EDS mapping images were taken for observing the distribution of Cu. The SEM-EDS spectrum (inset) showed the characteristic K_α-X-rays peak at 8.027 keV. The Cu element in the sample was mapped using such characteristic X-ray. The PVP-VP_n containing CuNPs presented the red dots dealing with Cu elements (Figure 4C(b)). Without the Cu element, the red dot was not found in the mapping image (Fig. 4C(a). The Cu mapping observed in the PVP-VP_n matrix agree with the Cu mapping as observed on the chitosan-graft-PE surface in the previous report (Pasanphan & Chirachanchai, 2008; Pasanphan, Haema, Tangthong, & Piroonpan, 2014)

Suan Sunandha Science and Technology Journal

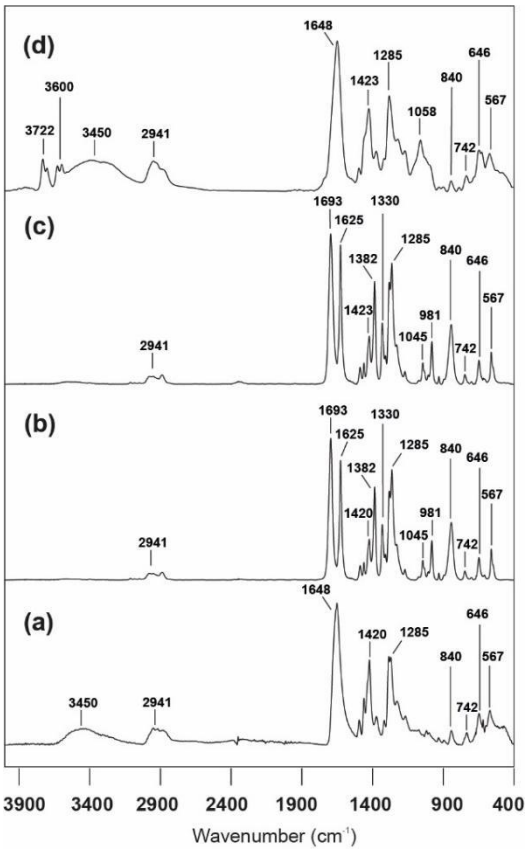

Figure 3. FT-IR spectra of (a) PVP, (b) VP, (c) PVP/VP mixture (ratio 40:60) and (d) irradiated PVP-VP_n (25 kGy).

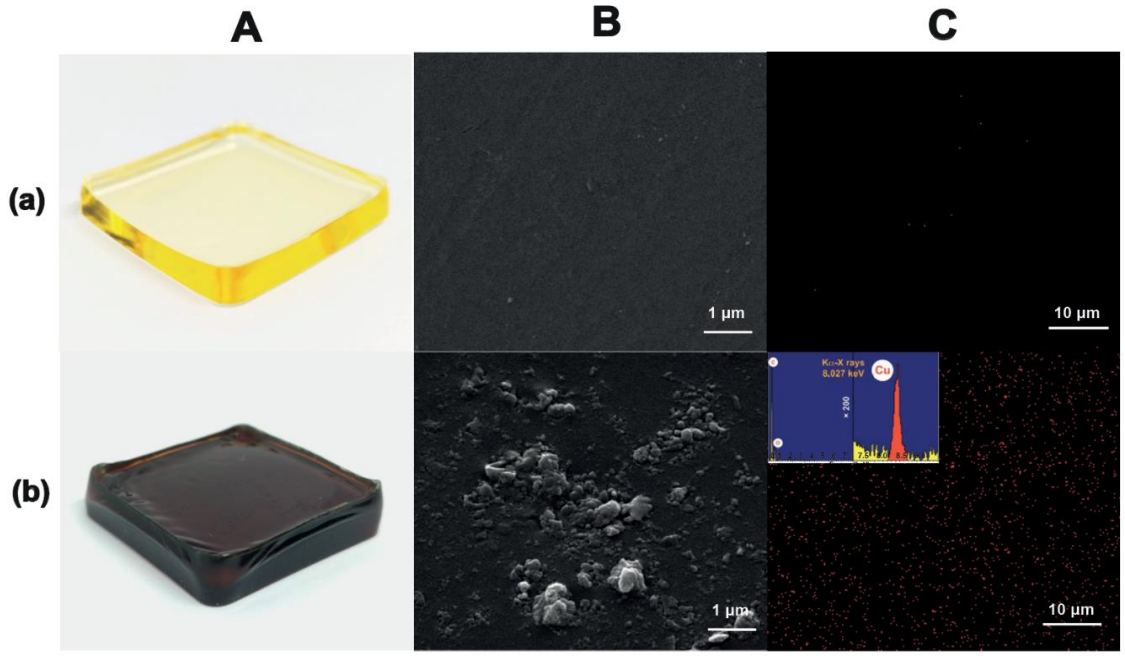

Figure 4. (A) Physical appearance, (B) SEM images, (C) SEM-EDS mapping and EDS spectrum (inset) of (a) PVP-VP and (b) CuNPs-PVP-VP_n composite material.

Suan Sunandha Science and Technology Journal

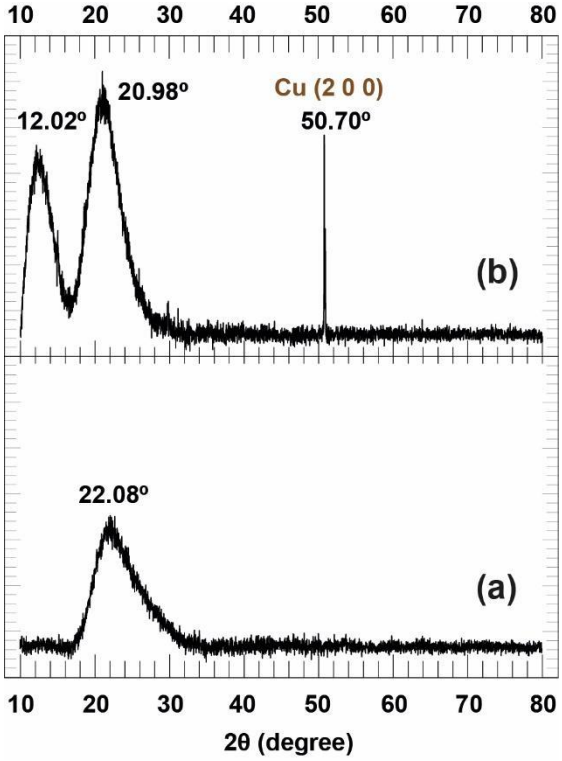

Figure 5. XRD patterns of (a) PVP-VP and (b) PVP-VP-Cu composite material.

3.5 Packing structure and crystal analysis

The XRD patterns of the PVP-VP_n and CuNPs-PVP-VP_n composite materials are shown in Figure 5. The broad diffraction peak at 22.08° (2θ) was observed for the PVP-VPn sample (Figure 5A). The diffraction peaks of PVP-VP_n were in agreement with pure PVP as in the previous literature (Vijaya, Selvasekarapandian, Nithya, & Sanjeeviraja, 2015). The diffraction peak was also observed between ~15°-30° which could be associated with the semi-crystallinity of pure PVP. For CuNPs-PVP-VP_n, the XRD pattern exhibited 2 board diffraction peaks at 12.02° (2θ) and 20.98° (2θ). These two peaks were interpreted as the crystalline of the PVP-VP_n polymeric matrix. The additional diffraction peak at 12.02°(2θ) might be due the new crystalline structure formed because of the influence of metal ions and CuNPs complex with the polymer chain. In addition, the main diffraction peak at 22.08° (2θ) of PVP-VP_n was also shifted to 20.98° (2θ). These changes indicate that the addition of CuNPs to the PVP-VP_n matrix reduced the crystalline nature of PVP-VP_n. This is due to the complexation between the host polymer PVP-VP_n and the CuNPs. It has been reported that when a polymer is complexed with a metal, salt or acid, the crystallinity of the polymer host could be disrupted by the addition of impurities (Kumar, Kim, Nahm, & Elizabeth, 2007).

In addition, the significant and sharp diffraction peak was observed at 50.70° (2θ) (Figure 5B). This new diffraction peak corresponds to (2 0 0) planes of CuNPs (Pham et al., 2012). The diffraction peak of CuNPs observed in PVP-VP_n sample also agreed with that of CuNPs as reported in the previous literature (Phul, Kaur, Farooq, & Ahmad, 2018). The XRD pattern confirmed the face centered cubic lattice of copper (Biçer & Şişman, 2010). The diffraction peak was in good agreement with the standard pattern for pure face centered cubic phase of CuNPs (JCPDS No. 01-1241 & 03-1005). No impurity peaks of CuO or Cu_2O were observed. The XRD result strongly supports the successful synthesis of CuNPs in the PVP-VP_n matrix.

3.6 Physical appearance and stability of CuNPs-PVP-VP_n composite materials

Figure 6 depicts physical appearance and stability of CuNPs-PVP-VP_n samples prepared from different conditions under air atmosphere at ambient temperature and pressure. The PVP-VP_n polymer matrix exhibited transparency matrix. For PVP-VP_n containing CuNPs, the samples changed from transparent appearance to light brown and dark brown colors depending on the concentration of $CuSO_4$ precursor. With higher $CuSO_4$ concentration from 0 to 40 mM, brown color was greater when the long chain PVP polymer was used. The long chain PVP could efficiently stabilize Cu^{2+} and exhibited as a protective polymer that not only stabilizing Cu^{2+} at the initial step but also stabilizing CuNPs after already prepared. It was also found that CuNPs in the PVP-VP_n matrix were very stable for more than 180 days and were greater when the long chain PVP polymer was used. The long chain PVP could efficiently stabilize Cu^{2+} and exhibited as a protective polymer that not only stabilizing Cu^{2+} at the initial step but also stabilizing CuNPs after already prepared. It was also found that CuNPs in PVP-VP_n matrix were very stable more than 180 days.

Suan Sunandha Science and Technology Journal

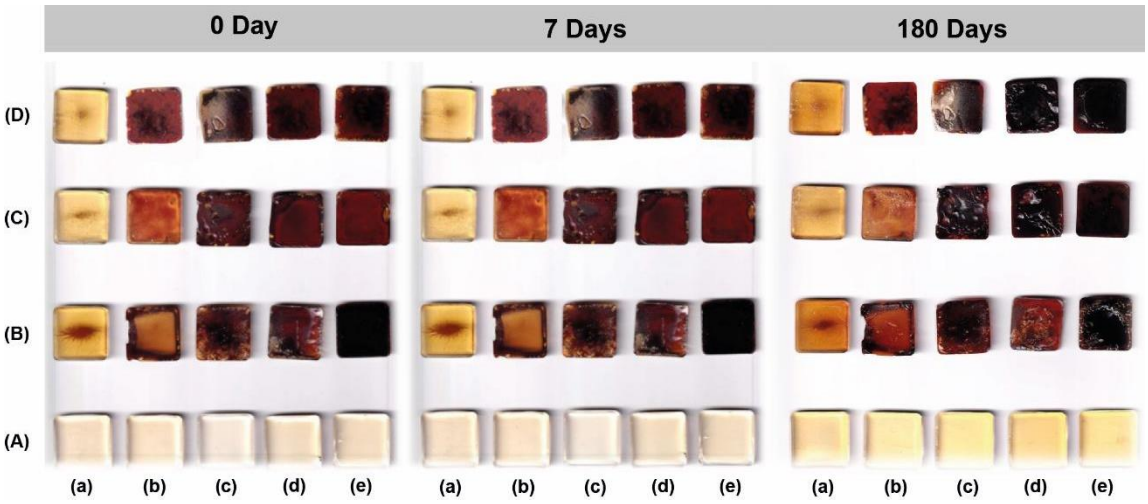

Figure 6. Physical appearances of CuNPs-PVP-VP_n composite material with $CuSO_4$ concentrations of (A) 0, (B) 10, (C) 20 and (D) 40 mM and PVP concentrations of (a) 0, (b) 10, (c) 20, (d) 30 and (e) 40% w/w in VP solution.

4. Conclusions

CuNPs-PVP-VP_n nanocomposite materials were successfully prepared using a simultaneous irradiation process based on radiation-induced reduction and polymerization/crosslinking mechanism. Gel fraction of PVP-VP_n polymer matrix was found when the PVP concentration of 0-20 %wt was used in VP monomer. Gel fraction of PVP-VP_n reduced with increasing PVP concentration. In the combination of PVP-VP_n and Cu ions precursor, CuNPs could successfully synthesize and stabilize in the PVP-VP_n material using irradiation technique with the dose of 25 kGy. CuNPs with the size of ca. 100 nm and some agglomerated CuNPs with the size of ca. 500 nm were embedded inside the PVP-VP_n polymer. The XRD diffraction peak indicated (2 0 0) plane of face centered cubic lattice of CuNPs confirmed successful synthesis of CuNPs without impurity. The CuNPs in PVP-VP_n composite material exhibited outstanding stability up to >180 days. Our established model process for the synthesis of CuNPs in solid polymer would be a practical process for further production of CuNPs for various industrial applications.

5. Acknowledgements

The authors (T.K. and W.P) appreciated Research and Researcher for Industries (RRI) (RRIMSD62_M1051), the National Research Council of Thailand (NRCT) (Thailand) for financial support of this research as a master degree project. The authors also acknowledge Coordinate Research Project (CRP) and Technical Cooperation Programme (THA1014), International Atomic Energy Agency (IAEA), United Nation (UN), Austria (Vienna) for supporting coordinate research and technical cooperation performed at the Center of Radiation Processing for Polymer Modification and Nanotechnology (CRPN), Faculty of Science, Kasetsart University (Thailand).

6. References

Ahmad, S. I. B., Ahmad, M. S. B. H., & Radiman, S. B. (2009). A study on gamma irradiation synthesis of copper nanoparticles. *AIP Conference Proceedings*, *1136*(1), 186-190. doi:10.1063/1.3160127

Alyan, A., Abdel-Samad, S., Massoud, A., & Waly, S. A. (2019). Characterization and thermal conductivity investigation of copper-polyaniline nano composite synthesized by gamma radiolysis method. *Heat and Mass Transfer*, *55*, 2409-2417. doi:10.1007/s00231-019-02588-z

Athanassiou, E. K., Grass, R. N., & Stark, W. J. (2006). Large-scale production of carbon-coated copper nanoparticles for sensor applications. *Nanotechnology*, *17*(6), 1668-1673. doi:10.1088/0957-4484/17/6/022

Suan Sunandha Science and Technology Journal

Biçer, M., & Şişman, İ. (2010). Controlled synthesis of copper nano/microstructures using ascorbic acid in aqueous CTAB solution. *Powder Technology*, *198*(2), 279-284. doi:10.1016/j.powtec.2009.11.022

Bondaz, L., Fontaine, P., Muller, F., Pantoustier, N., Perrin, P., Morfin, I., ... Cousin, F. (2020). Controlled synthesis of gold nanoparticles in copolymers nanomolds by X-ray radiolysis. *Langmuir*, *36*(22), 6132-6144. doi:10.1021/acs.langmuir.0c00554

Chandra, S., Kumar, A., & Tomar, P. K. (2014). Synthesis and characterization of copper nanoparticles by reducing agent. *Journal of Saudi Chemical Society*, *18*(2), 149-153. doi:10.1016/j.jscs.2011.06.009

Cheng, C., Li, J., Shi, T., Yu, X., Fan, J., Liao, G., ... & Tang, Z. (2017). A novel method of synthesizing antioxidative copper nanoparticles for high performance conductive ink. *Journal of Materials Science: Materials in Electronics*, *28*(18), 13556-13564. doi:10.1007/s10854-017-7195-9

Flores-Rojas, G. G., López-Saucedo, F., & Bucio, E. (2020). Gamma-irradiation applied in the synthesis of metallic and organic nanoparticles: A short review. *Radiation Physics and Chemistry*, *169*, 107962. doi:10.1016/j.radphyschem.2018.08.011

Giuffrida, S., Costanzo, L. L., Ventimiglia, G., & Bongiorno, C. (2008). Photochemical synthesis of copper nanoparticles incorporated in poly (vinyl pyrrolidone). *Journal of Nanoparticle Research*, *10*(7), 1183-1192. doi:10.1007/s11051-007-9343-2

Hiremath, P., Nuguru, K., & Agrahari, V. (2019). Material attributes and their impact on wet granulation process performance. In A. S. Narang, & S. Badawy (Eds.), *Handbook of pharmaceutical wet granulation* (pp. 263-315). Academic Press.

Hsu, S. L. C., & Wu, R. T. (2007). Synthesis of contamination-free silver nanoparticle suspensions for micro-interconnects. *Materials Letters*, *61*(17), 3719-3722. doi:10.1016/j.matlet.2006.12.040

Ismail, N. A., Shameli, K., Wong, M. M. T., Teow, S. Y., Chew, J., & Sukri, S. N. A. M. (2019). Antibacterial and cytotoxic effect of honey mediated copper nanoparticles synthesized using ultrasonic assistance. *Materials Science and Engineering: C*, *104*, 109899. doi:10.1016/j.msec.2019.109899

Jannoo, K., Teerapatsakul, C., Punyanut, A., & Pasanphan, W. (2015). Electron beam assisted synthesis of silver nanoparticle in chitosan stabilizer: Preparation, stability and inhibition of building fungi studies. *Radiation Physics and Chemistry*, *112*, 177-188. doi:10.1016/j.radphyschem.2015.03.035

Joshi, S. S., Patil, S. F., Iyer, V., & Mahumuni, S. (1998). Radiation induced synthesis and characterization of copper nanoparticles. *Nanostructured Materials*, *10*(7), 1135-1144. doi:10.1016/S0965-9773(98)00153-6

Koczkur, K. M., Mourdikoudis, S., Polavarapu, L., & Skrabalak, S. E. (2015). Polyvinylpyrrolidone (PVP) in nanoparticle synthesis. *Dalton Transactions*, *44*(41), 17883-17905. doi:10.1039/C5DT02964C

Kumar, G. G., Kim, P., Nahm, K. S., & Elizabeth, R. N. (2007). Structural characterization of PVdF-HFP/PEG/Al_2O_3 proton conducting membranes for fuel cells. *Journal of Membrane Science*, *303*(1-2), 126-131. doi:10.1016/j.memsci.2007.06.069

Meyre, M. E., Tréguer-Delapierre, M., & Faure, C. (2008). Radiation-induced synthesis of gold nanoparticles within lamellar phases. Formation of aligned colloidal gold by radiolysis. *Langmuir*, *24*(9), 4421-4425. doi:10.1021/la703650d

Misra, N., Biswal, J., Gupta, A., Sainis, J. K., & Sabharwal, S. (2012). Gamma radiation induced synthesis of gold nanoparticles in aqueous polyvinyl pyrrolidone solution and its application for hydrogen peroxide estimation. *Radiation Physics and Chemistry*, *81*(2), 195-200. doi:10.1016/j.radphyschem.2011.10.014

Moazzenchi, B., & Montazer, M. (2020). Click electroless plating and sonoplating of polyester with copper nanoparticles producing conductive fabric. *Fibers and Polymers*, *21*(3), 522-531. doi:10.1007/s12221-020-9664-7

Pasanphan, W., & Chirachanchai, S. (2008). Polyethylene film surface functionalized with chitosan via γ-ray irradiation in

aqueous system: An approach to induce copper (II) ion adsorptivity on PE. *Reactive and Functional Polymers*, *68*(8), 1231-1238. doi: 10.1016/j.reactfunctpolym.2008.05.006

Pasanphan, W., Haema, K., Tangthong, T., & Piroonpan, T. (2014). Modification of chitosan onto PE by irradiation in salt solutions and possible use as Cu^{2+} complex film for pest snail control. *Journal of Applied Polymer Science*, *131*(23), 41204. doi:10.1002/app.41204

Pham, L. Q., Sohn, J. H., Kim, C. W., Park, J. H., Kang, H. S., Lee, B. C., & Kang, Y. S. (2012). Copper nanoparticles incorporated with conducting polymer: Effects of copper concentration and surfactants on the stability and conductivity. *Journal of Colloid and Interface Science*, *365*(1), 103-109. doi:10.1016/j.jcis.2011.09.041

Phul, R., Kaur, C., Farooq, U., & Ahmad, T. (2018). Ascorbic acid assisted synthesis, characterization and catalytic application of copper nanoparticles. *Material Science & Engineering International Journal*, *2*(4), 90-94. doi:10.15406/mseij.2018.02.00040

Piroonpan, T., Katemake, P., & Pasanphan, W. (2020). Comparative study of different chitosan solutions to assist the green synthesis of gold nanoparticles under irradiation. *Radiation Physics and Chemistry*, *169*, 108250. doi:10.1016/j.radphyschem.2019.03.054

Pornpitchanarong, C., Rojanarata, T., Opanasopit, P., Ngawhirunpat, T., & Patrojanasophon, P. (2020). Synthesis of novel N-vinylpyrrolidone/acrylic acid nanoparticles as drug delivery carriers of cisplatin to cancer cells. *Colloids and Surfaces B: Biointerfaces*, *185*, 110566. doi:10.1016/j.colsurfb.2019.110566

Ramesh, S., Vetrivel, S., Suresh, P., & Kaviarasan, V. (2020). Characterization techniques for nano particles: A practical top down approach to synthesize copper nano particles from copper chips and determination of its effect on planes. *Materials Today: Proceedings*, *33*, 2626-2630. doi:10.1016/j.matpr.2020.01.157

Ramnani, S. P., Biswal, J., & Sabharwal, S. (2007). Synthesis of silver nanoparticles supported on silica aerogel using gamma radiolysis. *Radiation Physics and Chemistry*, *76*(8-9), 1290-1294. doi:10.1016/j.radphyschem.2007.02.074

Tangthong, T., Piroonpan, T., Thipe, V. C., Khoobchandani, M., Katti, K., Katti, K. V., & Pasanphan, W. (2021a). Bombesin peptide conjugated water-soluble chitosan gallate—A new nanopharmaceutical architecture for the rapid one-pot synthesis of prostate tumor targeted gold nanoparticles. *International Journal of Nanomedicine*, *16*, 6957-6981. doi:10.2147/IJN.S327045

Tangthong, T., Piroonpan, T., Thipe, V. C., Khoobchandani, M., Katti, K., Katti, K. V., & Pasanphan, W. (2021b). Water-soluble chitosan conjugated DOTA-Bombesin peptide capped gold nanoparticles as a targeted therapeutic agent for prostate cancer. *Nanotechnology, Science and Applications*, *14*, 69-89. doi:10.2147/NSA.S301942

Tomotoshi, D., & Kawasaki, H. (2020). Surface and interface designs in copper-based conductive inks for printed/flexible electronics. *Nanomaterials*, *10*(9), 1689. doi:10.3390/nano10091689

Vijaya, N., Selvasekarapandian, S., Nithya, H., & Sanjeeviraja, C. (2015). Proton conducting polymer electrolyte based on poly (N-vinyl pyrrolidone) doped with ammonium iodide. *International Journal of Electroactive Materials*, *3*, 20-27.

Wahyudi, S., Soepriyanto, S., & Mubarok, M. Z., & Sutarno. (2018). Synthesis and applications of copper nanopowder–A review. *IOPConference Series: Materials Science and Engineering*, *395*(1), 012014. doi:10.1088/1757-899X/395/1/012014

Wongkrongsak, S., Tangthong, T., & Pasanphan, W. (2016). Electron beam induced water-soluble silk fibroin nanoparticles as a natural antioxidant and reducing agent for a green synthesis of gold nanocolloid. *Radiation Physics and Chemistry*, *118*, 27-34. doi:10.1016/j.radphyschem.2015.03.020

Wongpisutpaisan, N., Charoonsuk, P., Vittayakorn, N., & Pecharapa, W. (2011). Sonochemical

Suan Sunandha Science and Technology Journal

synthesis and characterization of copper oxide nanoparticles. *Energy Procedia*, *9*, 404-409. doi:10.1016/j.egypro.2011.09.044

Zhou, F., Zhou, R., Hao, X., Wu, X., Rao, W., Chen, Y., & Gao, D. (2008). Influences of surfactant (PVA) concentration and pH on the preparation of copper nanoparticles by electron beam irradiation. *Radiation Physics and Chemistry*, *77*(2), 169-173. doi:10.1016/j.radphyschem.2007.05.007

Zinn, A. A., Stoltenberg, R. M., Fried, A. T., Chang, J., Elhawary, A., Beddow, J., & Chiu, F. (2012). Nanocopper based solder-free electronic assembly material. *Nanotech*, *2*, 71-74.